JACS
JOURNAL OF THE AMERICAN CHEMICAL SOCIETY

ARTICLE

pubs.acs.org/JACS

Controlled Assembly of Ag Nanoparticles and Carbon Nanotube Hybrid Structures for Biosensing

Sangeeta Sahoo,[*,∥,†] Sudhir Husale,[*,∥,‡] Shashi Karna,[⊥] Saroj K. Nayak,[¶] and Pulickel M. Ajayan[§]

[†]Department of Materials Science and Engineering, Rensselaer Polytechnic Institute, Troy, New York 12180, United States

[‡]Rowland Institute at Harvard, Harvard University, 100 Edwin H. Land Boulevard, Cambridge, Massachusetts 02142, United States

[⊥]AMSRD-ARL-WM-BD, Weapons & Materials Directorate, US Army Research Laboratory, Aberdeen Proving Ground, Maryland 21005-5069, United States

[¶]Department of Physics, Applied Physics and Astronomy, Rensselaer Polytechnic Institute, Troy, New York 12180, United States

[§]Department of Mechanical Engineering and Materials Science, Rice University, 6100 Main Street, Houston, Texas 77005, United States

Supporting Information

ABSTRACT: Here we report a chemical-free, simple, and novel method in which a part from a silver-based anode is controllably used in a straightforward manner to produce silver nanoparticles (Ag NPs) in order to fabricate a controlled assembly of Ag NPs and single walled carbon nanotube (SWCNT) hybrid structures. The attachment and distribution of Ag NPs along SWCNTs have been investigated and characterized by field emission scanning electron microscopy (FESEM). We have achieved the decoration of SWCNTs with different densities of Ag NPs by changing the deposition time, the applied voltage, and the location of carbon nanotubes with respect to the anode. At low voltage, single silver nanoparticle is successfully attached at the open ends of SWCNTs whereas at high voltage, intermediate and full coverage densities of Ag NPs are observed. As voltage is further increased, fractals of Ag NPs along SWCNTs are observed. In addition, a device based on a Ag NPs−SWNT hybrid structure is used for the label-free detection of ssDNA molecules immobilized on it. We believe that the proposed method can be used to decorate and/or assemble metal nanoparticles or fractal patterns along SWCNTs with different novel metals such as gold, silver, and copper and can be exploited in various sensitive applications for fundamental research and nanotechnology.

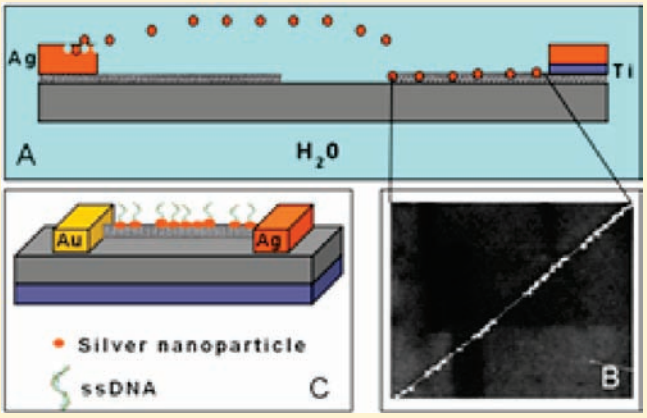

Metal decoration on nanotubes has opened a new avenue of research with significant opportunities in various fields.[1−10] One main purpose of the decoration of nanotubes is to make a sensitive hybrid device in which metal nanoparticles act as reactive sites for the adsorption of the chemical and/or biological species. In particular, the assembly of carbon nanotubes (CNTs) and silver nanoparticles (Ag NPs) has specific interest as a new hybrid material because its recent potential applications have been found useful in the study of SERS,[8,11] antimicrobial agents,[12] pH sensors,[13] gas sensors,[14] electrical conductivity enhancement,[15] electrocatalytic activity,[16] etc. Several methods of metal decoration on CNTs have been reported[17] and reviewed.[9,18] Electrodeposition is the most popular technique used so far for the selective decoration of nanoparticles along CNTs.[19−24] These methods decorate CNTs with metals but require the use of chemicals and/or catalysts. In this context, we report a new, simple, chemical- and catalyst-free technique providing different densities of Ag NPs on the SWCNT network that can be used to fabricate Ag NPs−SWNT-based hybrid nanostructures having potential use in various nanotechnological applications.

Our simple method to decorate SWCNTs is depicted schematically in Figure 1A and explained in Experimental Methods. At first, SWCNTs were grown on highly doped SiO_2/Si (100) wafers by a chemical vapor deposition method as described[25] and used[26] previously in our study. Figure 1B shows the pristine SWCNTs connected to the cathode during the nanoparticle deposition process. After an application of 500 mV potential between the electrodes for 19 min, the device was taken out of the DI water, dried under nitrogen gas, and subsequently imaged in FESEM. The corresponding Ag-decorated nanotubes are shown in Figure 1C. The images of SWCNTs before (Figure 1B) and after the deposition (Figure 1C) clearly

Received: October 16, 2010
Published: February 24, 2011

dx.doi.org/10.1021/ja1093327 | J. Am. Chem. Soc. 2011, 133, 4005–4009

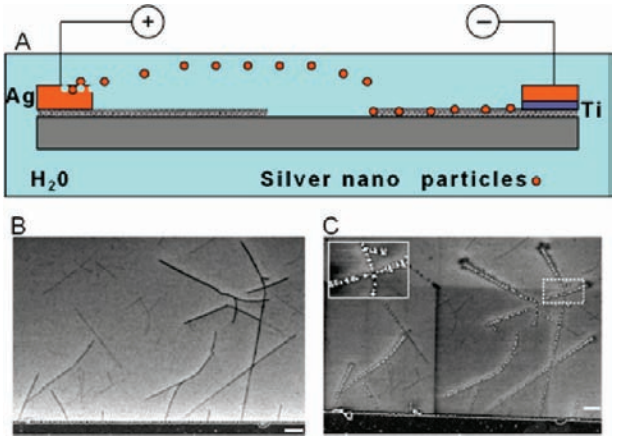

Figure 1. Attachment of silver nanoparticles on single walled carbon nanotubes. (A) A schematic presentation of silver nanoparticle (orange color) attachment under an electric field. FESEM micrographs representing the SWCNT network (B) before and (C) after the decoration with Ag NPs. Inset: The magnified image of the dotted rectangular portion in C. The scale bar represents 1 μm length.

demonstrate the proof of the principle of this method, indicating a selective decoration of SWCNTs with Ag NPs.

A single nanoparticle attachment at the tip of the SWCNT is observed at 250 mV as shown by a white dotted circle in Figure 2A. Here the distance between two electrodes was set to 100 μm. The potential was applied for 19 min. It is very likely to have a single particle decoration at the free end (where the electric field is high) of the SWCNT whose one end is clamped and connected to the cathode, which is described in Experimental Methods. In Figure 2B, one nanotube clearly shows the nanoparticle attachment at the tip whereas the other nanotube does not show any attachment of silver nanoparticle. This could be due to the broken connection of nanotubes. Here the electric field distribution between two metal electrodes in DI water influences as well as directs the nanoparticle attachment on the SWCNTs. Recently we have also observed that the electric field distribution between two electrodes play an important role in the growth of various Cu_2O nanostructures.[27]

To achieve an intermediate and full coverage of the decoration, we have increased the potential from 250 mV to 500 mV, keeping the deposition time the same (19 min) as it was for the attachment of a single particle. We have monitored the formation of the Ag NP assembly on SWCNTs at different places with respect to the electrodes. Because there are different nanotubes attached at different places of the cathode, the electric field distribution depends on the specific position of the SWCNTs with respect to the anode. Note that the cathode and the anode are of rectangular shapes (300×100 μm^2). Here the effective electric field plays an important role on the Ag NPs attachment to SWCNTs. In our results, geometry of the metal pads (electrodes) and the respective position of the nanotubes enable the different particle densities along the SWCNT. Figure 2C and 2D shows the coverage with a few particles along the SWCNTs. Note that these nanotubes were selected from the particular location where the density of Ag NPs was low. Also there is the possibility of semiconducting nanotubes in the SWCNT network that might show a relatively lower density of particles.

The above-mentioned device with the same parameters as in the case of medium coverage with Ag NPs also shows high coverage of particles as shown in Figure 2E and 2F. The high coverage with Ag NPs is observed near the cathode region (Figure 2E,F) facing to the anode. We have observed full coverage with silver particles, which is equivalent to a new class of hybrid materials composed of metallic nanowire and SWCNTs. More dense patterns were observed at the tip of the SWCNTs attached to the cathode (Figure 2E,F). Importantly, we observe that the nanotubes that are not connected to the electrodes remain unaffected by the decoration, confirming that the process is directed by the electric field. Figure 2C−F demonstrates that different particle densities can be obtained along the SWCNTs based on the distribution of electric field.

We also investigated the use of higher voltages on the decoration process of the SWCNT network. Higher external potential causes the Ag NP-based aggregates to grow into fractal patterns along the SWCNTs (Figure 3). The presence of SWCNTs can be observed in the fractal patterns as shown by the arrows in Figure 3B−E. Here Ag NPs form clusters of fractal patterns on the SWCNTs which act as dividers for the growth patterns, and the attached Ag NPs might act as the point of nucleation growth. Two types of fractal patterns were clearly visible as shown in Figure 3. The first type of patterns, shown in Figure 3A−C, was observed after the application of 1 V external potential during 10 min. Increased voltage causes a higher density of Ag NPs along the SWCNT, indicating a fast and multistep process. Consistent growth of these patterns was directed along the nanotubes, keeping the nanotubes at the center.

During the deposition, some Ag^+ ions also deposit at the Ag-cathode and nucleate to form nanoparticles. These freshly deposited Ag NPs at the Ag-cathode can be ejected back from the cathode to restore the anode by reversing the biases at the electrodes for a short duration. We found that these Ag NPs can also be utilized to form rapid and controlled assembly of fractal patterns along and around the SWCNTs. Fractal patterns thus formed are noted as the second type of patterns and are shown in Figure 3D−F. These patterns were formed by reversing the polarity of the electrodes of a sample that had undergone the intermediate coverage decoration process at 500 mV and the fractal formation for 10 s deposition time with 1.5 V reverse bias. These results demonstrate that the present approach can be used for the synthesis of Ag fractal patterns along the SWCNTs. Fractal patterns along SWCNTs can have useful applications in SERS-based sensors and detectors.

Finally, the Ag NP-decorated SWCNTs were used to fabricate two-terminal electrical devices for biosensing applications (Figure 4A). Current−voltage ($I-V$) measurements were carried out on the hybrid devices to probe the electrical detection of immobilized DNA molecules. We measured the $I-V$ characteristics for the device treated with (i) high salt buffer, (ii) DNA in high salt buffer, (iii) deionized water to rinse and clean, and (iv) DNA in hybridization buffer in order to rule out any changes in its resistance values due to the salt buffers only. The black curve in Figure 4D represents the electrical characterization of the as-fabricated hybrid device with a resistance of 170 kΩ prior to any treatment with DNA molecules. After incubation with high salt buffer only, the device was dried with nitrogen gas. The corresponding electrical response presented by the red curve shows an increase in the resistance to ~190 kΩ. The same device was again washed with DI water and treated with the thiolated ssDNA in high salt buffer. After a 2 h treatment, the device was dried with nitrogen gas and resistance was measured to be ~335 kΩ, as shown by the green curve. In order to determine the resistance due only to ssDNAs, the device was extensively

dx.doi.org/10.1021/ja1093327 |*J. Am. Chem. Soc.* 2011, 133, 4005–4009

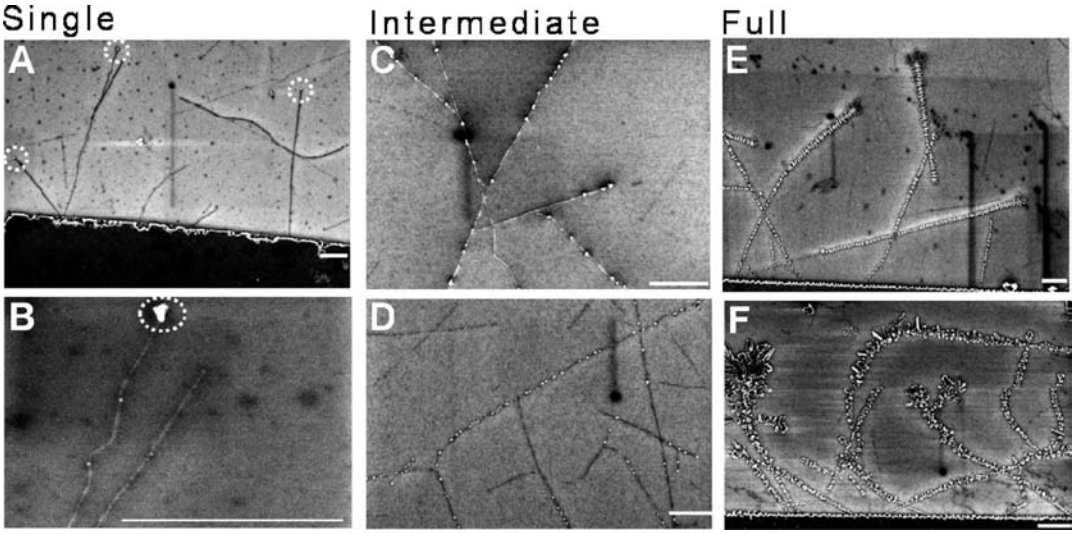

Figure 2. Controlled decoration with Ag NPs on SWCNTs. (A and B) Attachment of a single silver nanoparticle at the open end (unclamped) of SWCNTs. The circular dotted regions highlight the specific attachments. Intermediate decoration (C and D) and full coverage (E and F) with nanoparticles along SWCNTs. The scale bar represents 1 μm length.

washed with DI water and dried with nitrogen gas. Note that after the cleaning only thiolated DNA should be present on the device, whereas the nonspecifically bound DNA as well as the buffer salts should be removed. In this case we found the resistance value to be around 220 kΩ. We assumed that this value represents the device resistance with only ssDNA attached via the Ag NPs to the nanotube.

Additional experiments were performed with 1x SSC (saline−sodium citrate) hybridization buffer. The device was incubated in this buffer for 2 h and dried with nitrogen gas. The changes in electrical resistance are shown by the gray curve indicating (698 kΩ) a further increase in resistance as compared to the green curve measured with ssDNA under high salt buffer conditions. The device was rinsed carefully twice with DI water and dried with nitrogen gas. The measured electrical response on the washed device is shown by the cyan curve. Measured resistance of the device was ∼226 kΩ, which is very close to the resistance of the device with ssDNAs attached via Ag NPs alone above (220 kΩ, blue curve), confirming the label-free detection of ssDNA molecules immobilized on this hybrid device.

In conclusion, we have shown a controlled and selective decoration process of SWCNTs with Ag NPs by introducing a self-sacrificial layer-based technique and used it for the label-free detection of ssDNA molecules accurately under different buffer conditions. The approach represents a simple and catalyst- and chemical-free electrodepostion of Ag NPs on SWCNTs, leading to a clean, active surface at a predefined substrate location that can be potentially used in a wide variety of sensor and detector applications. Such hybrid/fully decorated SWCNTs can be used as metal nanowires for applications in biosensing or fractal formations. Further investigations of such nanobiohybrid devices coupled with microfluidics may provide more sensitive and specific approaches for DNA hybridization detection and real time detection of single base pair mismatches in liquid environments.

EXPERIMENTAL METHODS

Experimental Details. The size of the substrates was ∼8 × 8 mm^2. At a specific location, defined by the density of the SWCNT network, electrical pads were patterned by conventional lithography followed by the metallization using an e-beam deposition system. The electrodes are of rectangular shape with area ∼300 × 100 μm^2, thickness ∼100 nm. As in our previous study, we used deionized (DI) water (resistivity ∼18 MΩ-cm, 5 mL) as an electrolyte for the electrodeposition process. In this method, one end of the SWCNTs were electrically contacted by a 100 nm silver layer on top of an adhesion layer of 5 nm Ti. Here, SWCNTs were used as the template (defined as the cathode electrode) for the deposition, and an additional silver contact pad, defined as the anode electrode, served as the depot for the Ag NPs. Note that the silver anode used as a sacrificial layer, and only a small portion, was contributing to the metal decoration (Figure 1A), and we found that

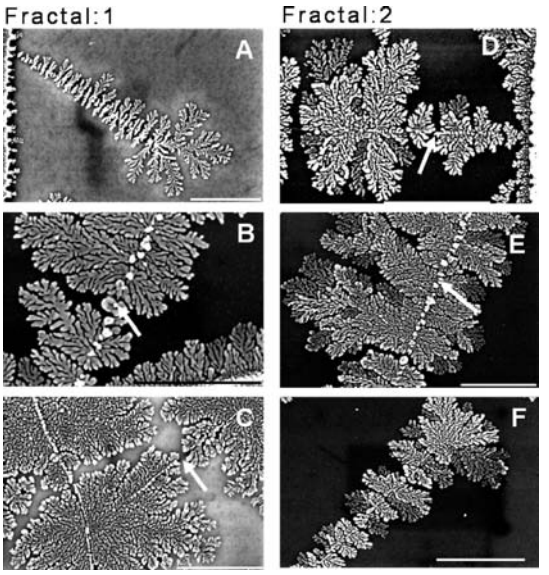

Figure 3. High coverage with Ag NPs along the SWCNTs. (A−C) FESEM images representing fractal nanopattern formation with Ag NPs along the SWCNT. (D and F) FESEM micrographs of two-dimensional fractal patterns. The arrows indicate the position of SWCNTs attached to the patterns. The scale bar represents 1 μm length.

dx.doi.org/10.1021/ja1093327 |J. Am. Chem. Soc. 2011, 133, 4005–4009

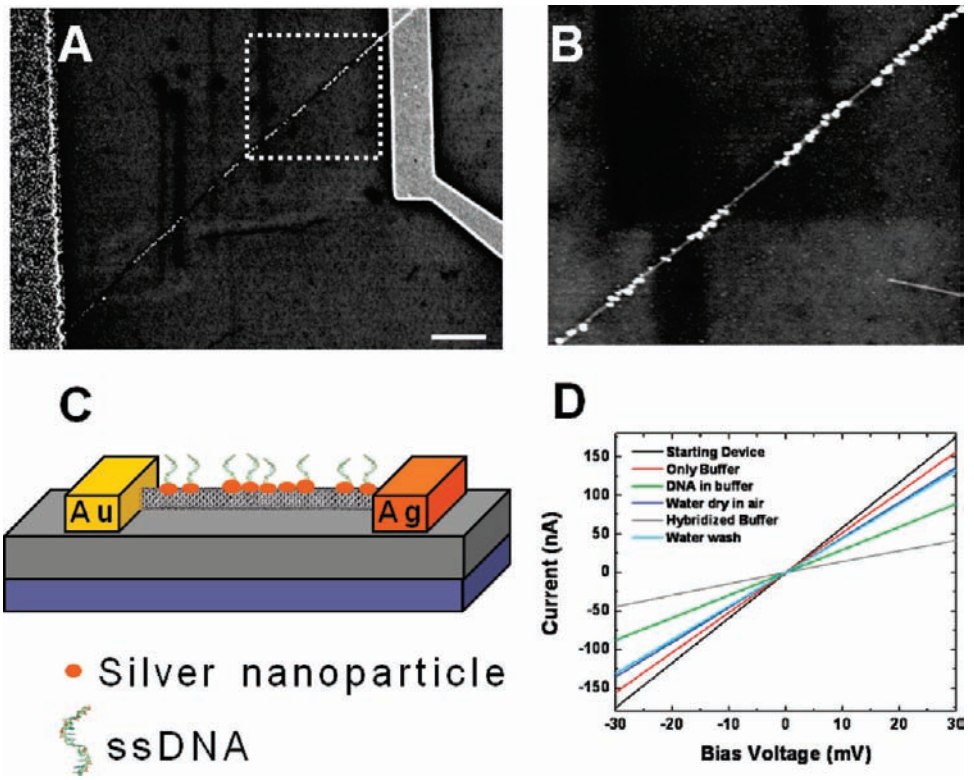

Figure 4. Biosensing with a Ag NPs-decorated SWCNT hybrid device. (A) FESEM micrograph of a Ag NPs−SWCNT-based hybrid two-terminal electrical device. (B) Zoomed image of the selected portion indicated by white dotted square region in A. (C) Schematics of immobilized ssDNA on Ag NPs−SWCNT-based hybrid devices. (D) The current−voltage ($I-V$) characteristics of the device under specific biological conditions (as indicated in the graph). The scale bar represents 1 μm length.

this metal layer was more than sufficient for the coating with Ag NPs at different densities on the SWCNT network.

Electrodeposition was carried out by applying a potential between two electrodes as explained above. The size of the electrodes and the distance between the two electrodes were kept constant while the potential was varied for the results presented in this study. A Karl-Suss micromanipulator accompanied by a Keithley 4200 source measure unit (SMU) was used for micromanipulation, contacting electrodes, and controlling voltages for the synthesis and also to measure the current−voltage characteristics in this study. Prior to inducing any voltage, the micromanipulator probes were connected to the pads of the sample that was immersed in DI water in order to connect cathode and anode.

Under an electric field in water at the positive terminal anode, silver atoms move out from the metal as Ag ions, leaving electrons in the electrode (Figure 1A). The difference in potential between the anode and cathode gives the driving force to these ions to flow from anode to cathode. The Ag ions released from the silver anode accumulate on the SWCNTs connected to the cathode where reduction occurs. Release of particles from the positive terminal depends on the applied potential and thus it affects the coverage with Ag NPs on the SWCNTs.

During SWCNT decoration with Ag NPs, we have observed that the coverage of particles depends on the distance between the two electrodes, applied bias voltage, deposition time, and the location of the SWCNTs attached to the cathode with respect to the anode. Different potentials were applied to achieve a very low density (one particle) to a very high density of nanoparticles. Rapid self-assembly of Ag NPs into a fractal pattern was observed at high voltages.

Biosensing Device Fabrication. The silver cathode already attached to one end of the hybrid structure was used as one of the metal contacts. The other contact was made by e-beam lithography followed by an e-beam deposition of a 100 nm Au layer on top of the 5 nm Ti layer. The Keithley SMU was used to measure the $I-V$ characteristics through the device. A newly fabricated hybrid device was incubated with a drop of ssDNA molecules for 2 h. Specific immobilization of thiolated ssDNA (sequence: 5′thiol_TCA TAC AGC TAG ATA ACC AAA GA) was carried out in high salt buffer, 1 M NaCl, phosphate buffer 10 mM, pH 7.4. In the incubation step, enough humidity was maintained to prevent the drop from drying.

■ ASSOCIATED CONTENT

Supporting Information. A table presenting the decoration time for forming various densities of Ag Nps along SWCNTs and an AFM image of a single nanoparticle-decorated SWCNT. This material is available free of charge via the Internet at http://pubs.acs.org.

■ AUTHOR INFORMATION

Corresponding Author

S.C.Husale@tnw.utwente.nl; san_sahoo@yahoo.com

Author Contributions

‖These authors contributed equally to this work.

■ ACKNOWLEDGMENT

Financial support was received from RPI, the IFC New York at RPI, Army Research Lab, and the NSF NSEC to pursue this work and is highly appreciated.

REFERENCES

(1) Planeix, J. M.; Coustel, N.; Coq, B.; Brotons, V.; Kumbhar, P. S.; Dutartre, R.; Geneste, P.; Bernier, P.; Ajayan, P. M. *J. Am. Chem. Soc.* **1994**, *116*, 7935–7936.

(2) Hu, J.; Ouyang, M.; Yang, P.; Lieber, C. M. *Nature* **1999**, *399*, 48.

(3) Kauffman, D. R.; Star, A. *Nano Lett.* **2007**, *7*, 1863–1868.

(4) Sun, Y.; Wang, H. H. *Adv. Mater.* **2007**, *19*, 2818–2823.

(5) Kong, J.; Chapline, M. G.; Dai, H. *Adv. Mater.* **2001**, *13*, 1384–1386.

(6) Byoung-Kye, K.; Noejung, P.; Pil Sun, N.; Hye-Mi, S.; Ju-Jin, K.; Hyojin, K.; Ki-Jeong, K.; Hyunju, C.; Beyong-Hwan, R.; Youngmin, C.; Jeong, O. L. *Nanotechnology* **2006**, 496.

(7) Jining, X.; Shouyan, W.; Aryasomayajula, L.; Varadan, V. K. *Nanotechnology* **2007**, 065503.

(8) Chen, Y.-C.; Young, R. J.; Macpherson, J. V.; Wilson, N. R. *J. Phys. Chem. C* **2007**, *111*, 16167–16173.

(9) Wildgoose, G. G.; Banks, C. E.; Compton, R. G. *Small* **2006**, *2*, 182–193.

(10) Zhao, Q.; Buongiorno Nardelli, M.; Lu, W.; Bernholc, J. *Nano Lett.* **2005**, *5*, 847–851.

(11) Kumar, R.; Zhou, H.; Cronin, S. B. *Appl. Phys. Lett.* **2007**, *91*, 223105.

(12) Yuan, W.; Jiang, G.; Che, J.; Qi, X.; Xu, R.; Chang, M. W.; Chen, Y.; Lim, S. Y.; Dai, J.; Chan-Park, M. B. *J. Phys. Chem. C* **2008**, *112*, 18754–18759.

(13) Zhao, L.; Shingaya, Y.; Tomimoto, H.; Huang, Q.; Nakayama, T. *J. Mater. Chem.* **2008**, *18*, 4759–4761.

(14) Espinosa, E. H.; Ionescu, R.; Bittencourt, C.; Felten, A.; Erni, R.; Van Tendeloo, G.; Pireaux, J. J.; Llobet, E. *Thin Solid Films* **2007**, *515*, 8322.

(15) Ma, P. C.; Tang, B. Z.; Kim, J.-K. *Carbon* **2008**, *46*, 1497.

(16) Yang, G.-W.; Gao, G.-Y.; Wang, C.; Xu, C.-L.; Li, H.-L. *Carbon* **2008**, *46*, 747.

(17) Jiang, K.; Eitan, A.; Schadler, L. S.; Ajayan, P. M.; Siegel, R. W.; Grobert, N.; Mayne, M.; Reyes-Reyes, M.; Terrones, H.; Terrones, M. *Nano Lett.* **2003**, *3*, 275–277.

(18) Georgakilas, V.; Gournis, D.; Tzitzios, V.; Pasquato, L.; Guldi, D. M.; Prato, M. *J. Mater. Chem.* **2007**, *17*, 2679–2694.

(19) Quinn, B. M.; Dekker, C.; Lemay, S. G. *J. Am. Chem. Soc.* **2005**, *127*, 6146–6147.

(20) Day, T. M.; Unwin, P. R.; Macpherson, J. V. *Nano Lett.* **2007**, *7*, 51–57.

(21) Day, T. M.; Unwin, P. R.; Wilson, N. R.; Macpherson, J. V. *J. Am. Chem. Soc.* **2005**, *127*, 10639–10647.

(22) Franklin, A. D.; Smith, J. T.; Sands, T.; Fisher, T. S.; Choi, K.-S.; Janes, D. B. *J. Phys. Chem. C* **2007**, *111*, 13756–13762.

(23) Qian, P.; Wu, Z.; Diao, P.; Zhang, G.; Zhang, J.; Liu, Z. *J. Phys. Chem. C* **2008**, *112*, 13346–13348.

(24) Quinn, B. M.; Lemay, S. G. *Adv. Mater.* **2006**, *18*, 855–859.

(25) Lastella, S.; Yang, H.; Rider, D.; Manners, I.; Ajayan, P., M.; Ryu, C. Y. *J. Polymer Sci., Part B: Polym. Phys.* **2007**, *45*, 758–765.

(26) Sahoo, S.; Maranganti, R.; Lastella, S.; Mallick, G.; Karna, S.; Sharma, P.; Ajayan, P. M. *Appl. Phys. Lett.* **2008**, *93*, 083120.

(27) Sahoo, S.; Husale, S.; Colwill, B.; Lu, T.-M.; Nayak, S.; Ajayan, P. M. *ACS Nano* **2009**, *3*, 3935–3944.